doi:10.1093/jmcb/mjab033
Published online May 28, 2021

Article

PSA controls hepatic lipid metabolism by regulating the NRF2 signaling pathway

Bangliang Huang[1,†], Xin Xiong[1,†], Linlin Zhang[1,†], Xiufei Liu[1], Yuren Wang[1], Xiaoli Gong[1], Qian Sang[1], Yongling Lu[2], Hua Qu[1,*], Hongting Zheng[1,*], and Yi Zheng [1,*]

[1] Department of Endocrinology, Translational Research of Diabetes Key Laboratory of Chongqing Education Commission of China, The Second Affiliated Hospital of Army Medical University, Chongqing, China
[2] Medical Research Center, Southwest Hospital of Army Medical University, Chongqing, China
[†] These authors contributed equally to this work.
[*] Correspondence to: Hua Qu, E-mail: quhuahua120@163.com; Hongting Zheng, E-mail: fnf7703@hotmail.com; Yi Zheng, E-mail: cecilia.zy@163.com

Edited by Feng Liu

The activity of proteinase is reported to correlate with the development and progression of nonalcoholic fatty liver disease (NAFLD). Puromycin-sensitive aminopeptidase (PSA/NPEPPS) is an integral nontransmembrane enzyme that functions to catalyze the cleavage of amino acids near the N-terminus of polypeptides. A previous study suggested that this enzyme acts as a regulator of neuropeptide activity; however, the metabolic function of this enzyme in the liver has not been explored. Here, we identified the novel role of PSA in hepatic lipid metabolism. Specifically, PSA expression was lower in fatty livers from NAFLD patients and mice (HFD, *ob/ob*, and *db/db*). PSA knockdown in cultured hepatocytes exacerbated diet-induced triglyceride accumulation through enhanced lipogenesis and attenuated fatty acid β-oxidation. Moreover, PSA mediated activation of the master regulator of antioxidant response, nuclear factor erythroid 2-related factor 2 (NRF2), by stabilizing NRF2 protein expression, which further induced downstream antioxidant enzymes to protect the liver from oxidative stress and lipid overload. Accordingly, liver-specific PSA overexpression attenuated hepatic lipid accumulation and steatosis in *ob/ob* mice. Furthermore, in human liver tissue samples, decreased PSA expression correlated with the progression of NAFLD. Overall, our findings suggest that PSA is a pivotal regulator of hepatic lipid metabolism and its antioxidant function occurs by suppressing NRF2 ubiquitination. Moreover, PSA may be a potential biomarker and therapeutic target for treating NAFLD.

Keywords: PSA, NAFLD, lipogenesis, fatty acid β-oxidation, NRF2

Introduction

Nonalcoholic fatty liver disease (NAFLD) is recognized as the most common liver disease, and almost 30% of people have been reported to be affected worldwide (Adams et al., 2005; Kawano and Cohen, 2013). It encompasses a pathophysiological spectrum of conditions, from simple steatosis to nonalcoholic steatohepatitis (NASH), further progression to fibrosis, cirrhosis, and ultimately liver carcinoma (Clark, 2006; Anstee et al., 2013). The phenotype and progression of NAFLD are determined by interactions between the environment and a susceptible polygenic host background, and no drug treatment is currently approved for NAFLD. With a high risk of liver-related morbidity and mortality along with metabolic comorbidities, understanding the mechanisms leading to NAFLD and enabling the development of novel therapeutic approaches have become a priority.

Reactive oxygen species (ROS) production has been implicated in the early stages of NAFLD due to increased liver fat load from the periphery (Koliaki et al., 2015). The excessive production of ROS impairs oxidative phosphorylation (OXPHOS) and β-oxidation, thereby promoting mitochondrial dysfunction and perpetuating the continued progression of NAFLD (Pessayre, 2007; Petrosillo et al., 2007). As a well-known master regulator of redox homeostasis, nuclear factor erythroid 2-related factor 2 (NRF2) is considered one of the major transcription factors involved in defense against oxidative stress (Hayes and Dinkova-Kostova, 2014; Vomund et al.,

Received December 23, 2020. Revised February 26, 2021. Accepted March 30, 2021.

2017). Under physiological conditions, NRF2 is targeted for proteasomal degradation via its association with Kelch-like ECH-associated protein-1. Upon oxidative stress, NRF2 dissociates from the complex and translocates into the nucleus, where it binds to the antioxidant responsive element (ARE) to initiate the antioxidant response. Thus, the regulation of NRF2 activity appears to be crucial for NAFLD development; however, the exact homeostatic mechanism remains partially unknown.

Puromycin-sensitive aminopeptidase (PSA, encoded by the NPEPPS gene), located in both the cytoplasm and cellular membranes, is a key zinc metallopeptidase belonging to the oxytocinase subfamily of the M1 aminopeptidase family that hydrolyzes amino acids from the N-terminus of its substrate (Constam et al., 1995; Gil et al., 2020). As a highly conserved protein, PSA is ubiquitously expressed in multiple tissues, and a previous genomic approach suggested its association with some human diseases, especially in the brain. For instance, PSA was found to be upregulated in human pineal parenchymal tumors and in medulloblastomas (Champier et al., 2005); it was also identified as a regulator of tau-induced Alzheimer's disease (Karsten et al., 2006), and its capability to protect against amyotrophic lateral sclerosis was exerted through attenuating oxidative stress (Ren et al., 2011). Recently, PSA has been reported to be involved in adipocyte dysfunction (Alponti et al., 2016). Currently, few studies have reported the role of PSA in the liver and lipid homeostasis; therefore, the physiological role of PSA in hepatocyte function, as well as in the development and progression of NAFLD, is of great interest.

In the present study, we provided evidence for the downregulation of hepatic PSA in both NAFLD patients and mouse models. PSA deficiency enhanced oxidative stress by promoting ubiquitination of NRF2 and resulted in enhanced lipid overload by stimulated lipogenesis and suppressed fatty acid β-oxidation. Moreover, rescue of PSA attenuated hepatic steatosis in a genetically induced (*ob/ob*) fatty liver model. Furthermore, in human liver tissue samples, decreased PSA expression correlated with the progression of fatty liver diseases, indicating a potential target for NAFLD.

Results

PSA expression is downregulated in the liver of NAFLD patients and mice

To investigate the possible association between PSA and liver lipid metabolism, we first observed hepatic PSA expression in HFD and genetically induced (*ob/ob* and *db/db*) NAFLD mouse models. Using quantitative real-time polymerase chain reaction (qRT-PCR), western blotting, and immunohistochemical (IHC) analyses, we showed that both the mRNA and protein levels of PSA were decreased in the liver of HFD model mice compared with mice fed normal chow (NC), with an inverse correlation to the induction of fatty acid synthase (FASN), an indicator of liver steatosis (Figure 1A). A reduction in PSA was also observed in the liver of *ob/ob* and *db/db* mice relative to the corresponding control (Figure 1B and C). Moreover, the mRNA and protein levels of PSA were reduced in the liver of NAFLD patients (ChiCTR-ROC-17010719, Figure 1D), which was consistent with the observations in mouse models. The shared downregulation of PSA expression observed in NAFLD patients and mice indicates a potential involvement of PSA in hepatic lipid metabolism and steatosis.

Knockdown of PSA exacerbates triglyceride accumulation by regulating both fatty acid synthesis and β-oxidation

To explore the possibility of PSA in hepatic lipid metabolism, we regulated PSA expression by inhibition or overexpression in Huh7 hepatocytes. Oil red O staining showed that lipid droplets were enhanced by PSA siRNA, but attenuated when PSA was overexpressed under free fatty acid (FFA) treatment but not under basal conditions (Figure 2A). Consistent changes in the triglyceride (TG) contents following PSA expression perturbation were also identified (Figure 2B). TG accumulation is considered as the major contributor to liver steatosis (Donnelly et al., 2005), and TG metabolism generally includes lipogenesis, fatty acid β-oxidation, fatty acid uptake, and lipid transport (Utzschneider and Kahn, 2006). Thus, we sought to determine the aspects of TG metabolism process that were modulated by PSA. As shown in Figure 2C, PSA primarily regulated the expression of lipogenic genes, such as sterol regulatory element-binding protein-1c (SREBP-1c), peroxisome proliferator-activated receptor-γ (PPARγ), and FASN, as well as genes encoding fatty acid β-oxidation, including peroxisome proliferator-activated receptor-γ coactivator-1α (PGC1α), acyl-CoA oxidase 1 (ACOX1), and carnitine palmitoyltransferase-1α (CPT-1α), rather than the genes related to fatty acid uptake and lipid transport (Figure 2C). Furthermore, the protein expression of fatty acid synthesis (nSREBP-1 and FASN) and β-oxidation (PGC1α) was also changed by PSA manipulation (Figure 2D). These findings suggest that PSA regulates hepatic TG metabolism by modulating lipogenesis and fatty acid β-oxidation. Moreover, we analyzed how mitochondria changed in the presence of PSA overexpression or knockdown. The number of mitochondria determined using MitoTracker staining and the mitochondrial DNA (mtDNA) content/total DNA ratio, as well as mitochondrial functions such as oxygen consumption rate (OCR) and OXPHOS, were measured. Consistent with the decreased PGC1α, which is also a marker of mitochondrial biogenesis (Liu et al., 2018), PSA knockdown resulted in repressed mitochondrial mass, mitochondrial respiration, and enzymatic activities of the OXPHOS complexes (Figure 2E–H). In contrast, overexpressing PSA in cultured hepatocytes enhanced mitochondrial biogenesis and metabolism compared to the Oe-control group (Figure 2E–H).

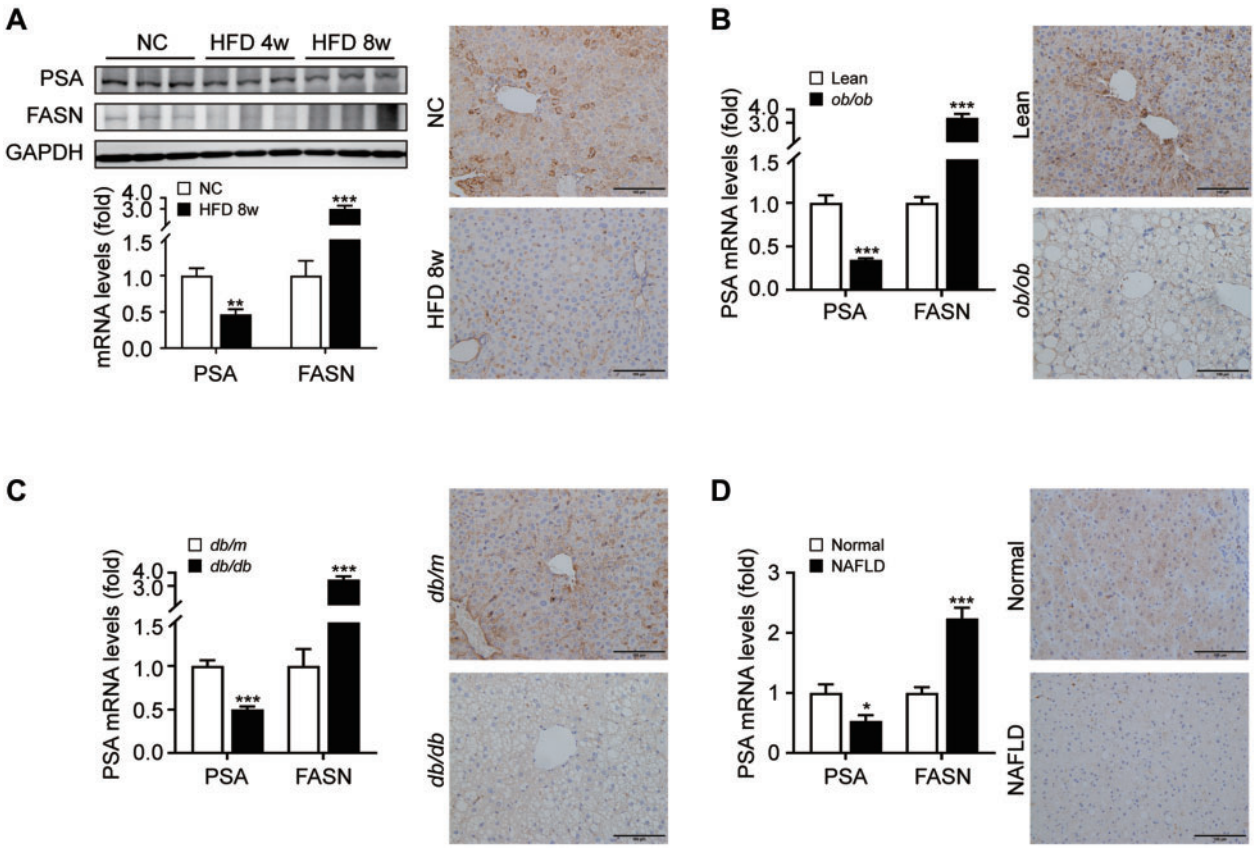

Figure 1 PSA is inhibited in fatty livers of mice and patients. (**A**) The mRNA and protein levels of hepatic PSA in HFD-fed mice at indicated time points. (**B**–**D**) The mRNA and protein levels of hepatic PSA in *ob/ob* mice (**B**), *db/db* mice (**C**), and NAFLD patients (**D**). Scale bar, 100 μm. $n = 5$ mice per group for **A**; $n = 6$ mice or patients per group for **B**–**D**. Data are presented as mean ± SEM. $^{*}P < 0.05$, $^{**}P < 0.01$, $^{***}P < 0.001$.

PSA regulates the NRF2 signaling pathway

Next, we explored the underlying molecular mechanisms of the effects of PSA, and several common factors related to liver lipid metabolism were subsequently assessed, such as endoplasmic reticulum (ER) stress, insulin signaling, and oxidative stress (Samuel and Shulman, 2012; Baiceanu et al., 2016; Mansouri et al., 2018). PSA absence did not significantly affect the mRNA levels of ER stress markers or the insulin signaling pathway (Supplementary Figure S1A and B), but it obviously induced the production of ROS under FFA treatment, as evidenced by both MitoSOX staining and flow cytometry assays (Figure 3A and B), and decreased the reduced form of glutathione to oxidized glutathione (GSH/GSSG) ratio (Figure 3C); in contrast, PSA overexpression reduced ROS and enhanced the ratio of GSH/GSSG (Figure 3A–C). In addition, we challenged hepatocytes with H_2O_2 and found that while 0.5 mM H_2O_2 did not induce a measurable amount of ROS in hepatocytes, it significantly increased the level of ROS in PSA-absent cells (Figure 3D). These results suggest that PSA might regulate oxidative stress in hepatocytes. ROS concentrations are commonly suppressed by activation of the transcription factor NRF2 and subsequent expression of antioxidant systems. Since NRF2 has also been reported to influence hepatic lipid metabolism (Bricambert et al., 2018; Azzimato et al., 2020), we next measured the mRNA and protein expression of the NRF2 pathway components under PSA modulation. The results showed that PSA altered the mRNA expression of NRF2 target genes, such as heme oxygenase-1 (HO-1), NAD(P)H quinone oxidoreductase 1 (NQO1), and glutamate–cysteine ligase modifier subunit (GCLM), without significantly affecting the transcription of NRF2 (Figure 3E), indicating that PSA most likely activated NRF2 target genes through upregulation of NRF2 at the protein level. This phenomenon was confirmed by immunoblotting analysis, which showed that ectopic expression of PSA significantly enhanced the levels of NRF2 and its downstream targets, which were inhibited when treated with PSA siRNA (Figure 3F). Collectively, these results suggest that PSA activates NRF2 to increase intracellular antioxidants in hepatocytes.

PSA effects occur via NRF2 control of the antioxidant response

To investigate the contribution of NRF2 to the protective effects of PSA, hepatocytes were cotransfected with PSA overexpression plasmid and NRF2 siRNA and treated with FFA. In

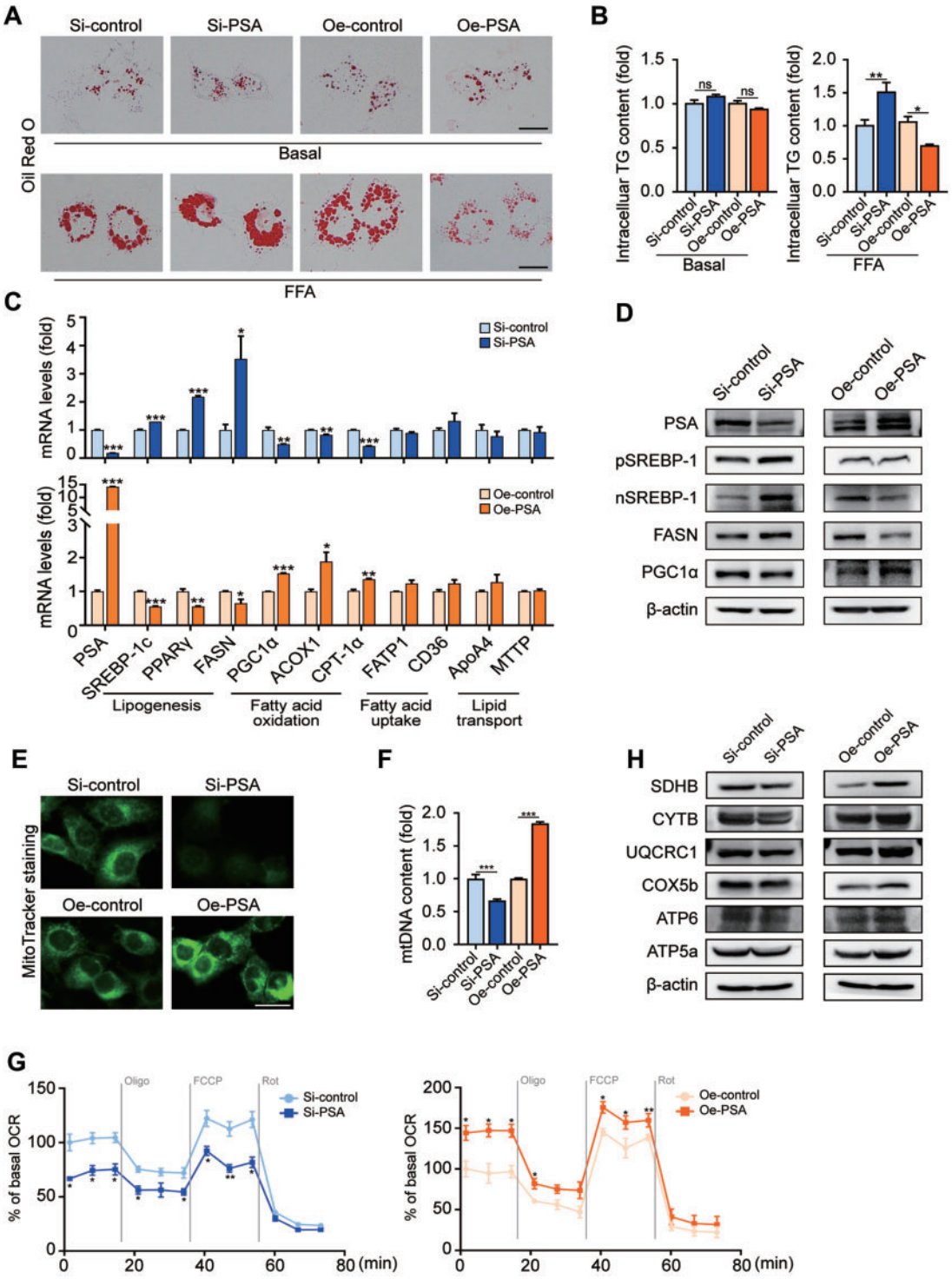

Figure 2 PSA suppresses hepatic fatty acid synthesis and induces β-oxidation. Huh7 hepatocytes were transfected with siRNA for PSA inhibition or plasmid for PSA overexpression, and then treated with or without FFAs for 24 h. (**A**) Oil red O staining. (**B**) TG content was determined enzymatically. (**C** and **D**) The mRNA and protein levels of indicated genes related to lipid metabolism were determined by qRT-PCR and western blotting. (**E**–**H**) MitoTracker staining (**E**), mtDNA content (**F**), Seahorse OCR (**G**), and protein levels of the OXPHOS complexes (**H**) were determined. Scale bar, 20 μm. $n = 3$. Data are presented as mean ± SEM. $^{*}P < 0.05$, $^{**}P < 0.01$, $^{***}P < 0.001$.

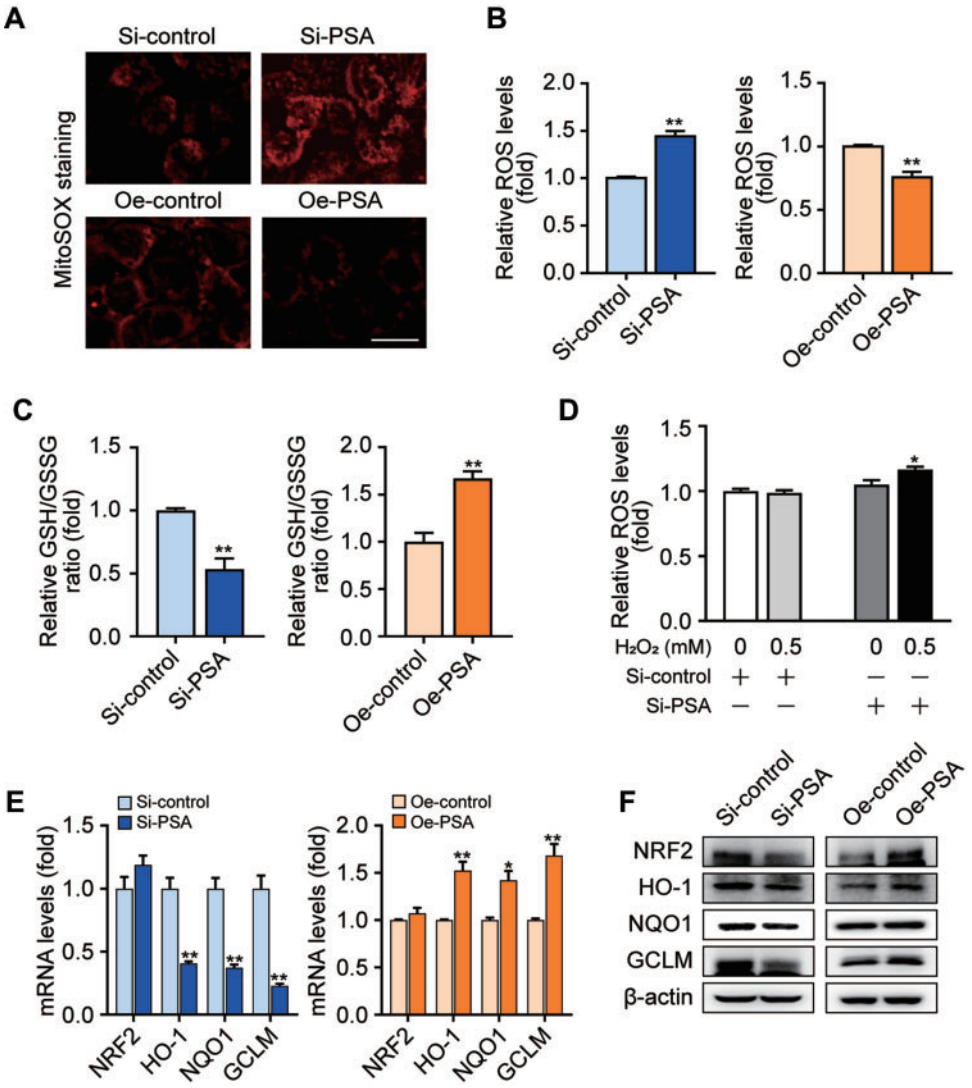

Figure 3 PSA upregulates the NRF2 signaling pathway. (**A**–**C**) Huh7 hepatocytes were transfected with siRNA for PSA inhibition or plasmid for PSA overexpression, and then treated with FFAs for 24 h. (**A** and **B**) ROS generation were determined by MitoSOX staining (**A**) and flow cytometry assay (**B**). (**C**) GSH/GSSG ratio was measured. (**D**) Huh7 hepatocytes transfected with PSA or control siRNA were treated with the indicated doses of H_2O_2 for 12 h. Intracellular ROS levels were measured by flow cytometry method. (**E** and **F**) The mRNA and protein levels of indicated genes related to the NRF2 signaling pathway were determined by qRT-PCR and western blotting. Scale bar, 20 μm. $n = 3$. Data are presented as mean ± SEM. $^*P < 0.05$, $^{**}P < 0.01$.

NRF2 knockdown cells, PSA transfection no longer induced the antioxidative gene HO-1 and the fatty acid β-oxidation gene PGC1α compared with the control, and PSA-inhibited expression of the lipogenic genes SREBP-1c and PPARγ and intracellular ROS generation were abrogated by NRF2 siRNA application (Figure 4A–C), indicating that NRF2 was necessary for PSA-regulated antioxidative response and lipid metabolism. Moreover, the protective effects of PSA on TG content and lipid droplet accumulation were abolished by NRF2 knockdown (Figure 4D and E). In addition, NRF2 siRNA negated the enhanced mitochondrial amount and function induced by PSA (Figure 4F–I). Overall, these results suggest that PSA abates ROS and alters hepatic lipid metabolism by activating NRF2 and downstream antioxidants.

PSA decreases the ubiquitination of NRF2, leading to an increase in NRF2 stability

We further explored the mechanism of PSA regulation of NRF2. Given that NRF2 was posttranscriptionally modulated by PSA (see Figure 3E and F), we first examined whether these interactions were endogenous. Immunoprecipitation analysis

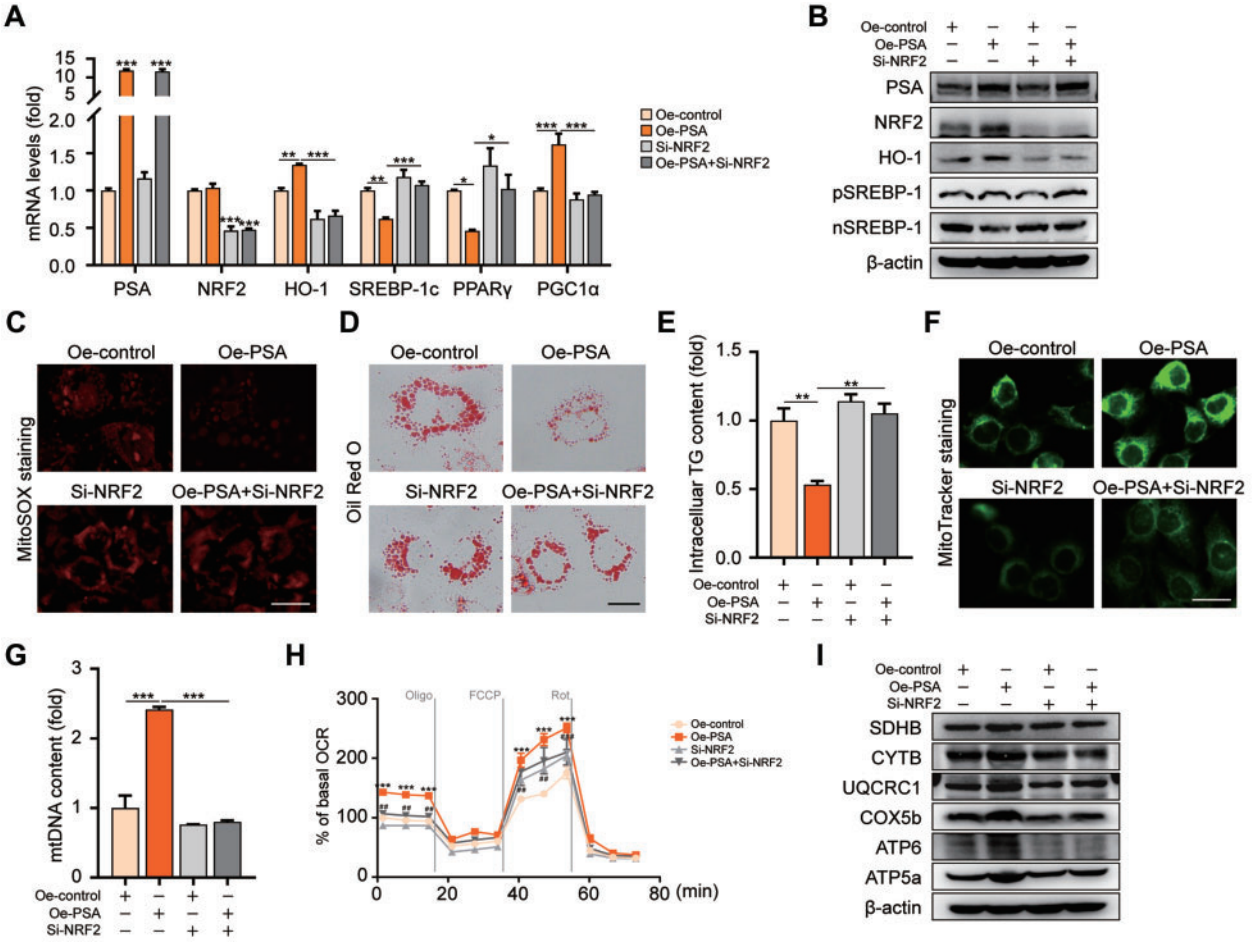

Figure 4 PSA attenuates lipid accumulation through inducing the NRF2 antioxidant response. Huh7 hepatocytes cotransfected with PSA plasmid and NRF2 siRNA were treated by FFAs for 24 h. (**A** and **B**) The mRNA and protein levels of indicated genes related to the NRF2 signaling pathway were determined. (**C**) ROS generation was determined by MitoSOX staining. (**D**) Lipid accumulation were determined by Oil red O staining. (**E**) TG content was determined enzymatically. (**F**) MitoTracker staining. (**G**) mtDNA content. (**H**) Seahorse OCR. (**I**) The protein levels of the OXPHOS complexes were determined. Scale bar, 20 μm. $n = 3$. Data are presented as mean ± SEM. $^{*}P < 0.05$, $^{**}P < 0.01$, $^{***}P < 0.001$.

was performed, and the results revealed an antibody against NRF2-precipitated PSA but not the IgG negative control (Figure 5A), indicating an endogenous interaction of PSA with NRF2. PSA has previously been reported to be involved in proteasomal degradation (Bhutani et al., 2007), and we next assessed the possibility that PSA could upregulate NRF2 via the ubiquitin–proteasome degradation pathway. The results showed that in hepatocytes with PSA overexpression, ubiquitinated NRF2 was significantly decreased (Figure 5B), while increased NRF2 ubiquitination was observed in PSA knockdown cells (Figure 5C). Moreover, the half-life of NRF2 was determined in the presence of PSA siRNA by cycloheximide (CHX) and immunoblotting analysis, and the results showed a decreased half-life of NRF2 with the application of PSA siRNA (Figure 5D). These data indicate that PSA stabilizes NRF2 and therefore activates the NRF2-mediated antioxidant response.

Rescue of PSA alleviates hepatic steatosis in genetically induced ob/ob mice

Next, we evaluated the effects of rescuing PSA expression in reversing its reduction observed during disease, and a liver-targeted therapeutic gene vector AAV8 was generated (Gao et al., 2002). Indeed, AAV8-PSA treatment led to PSA overexpression exclusively in the liver (Supplementary Figure S2). AAV8-PSA significantly reduced the ratio of liver weight to body weight (LW/BW), hepatic TG content, and serum low-density lipoprotein cholesterol (LDL) in *ob/ob* mice (Figure 6A–C). Moreover, the liver enzyme activities of alanine aminotransferase (ALT) and aspartate aminotransferase (AST) were also decreased (Figure 6D), indicating that liver functions were improved by AAV8-PSA. Accordingly, hepatic steatosis, lipid droplet accumulation, and ROS levels confirmed by histology, Oil red O, and MitoSOX staining were markedly attenuated in AAV8-PSA *ob/ob*

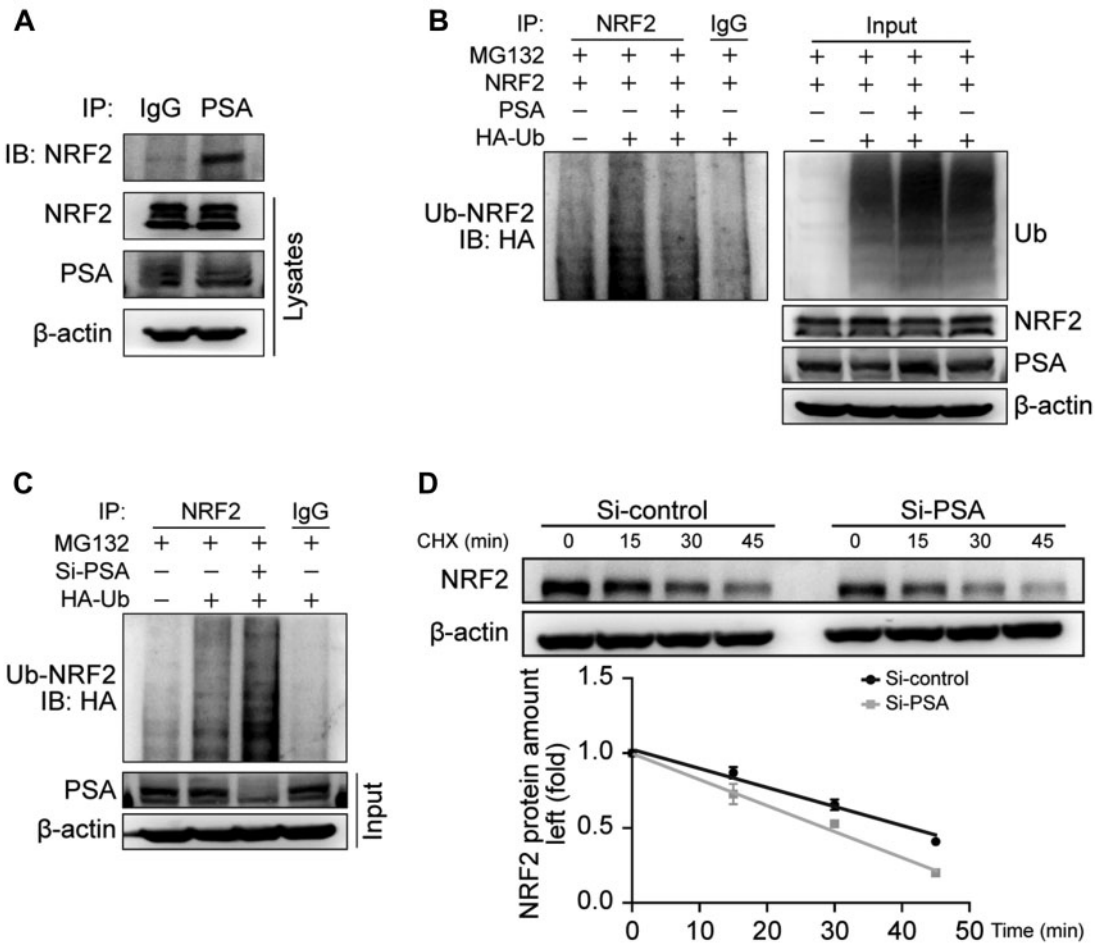

Figure 5 PSA decreases ubiquitination of NRF2, leading to an increase in NRF2 stability. (**A**) Cell lysates from Huh7 hepatocytes were immunoprecipitated (IP) using an antibody against PSA or IgG (negative control). The resulting immunoprecipitates were subjected to SDS–PAGE and analyzed by immunoblotting with a NRF2 antibody. (**B** and **C**) Huh7 hepatocytes were transfected by HA-tagged ubiquitin (Ub) and indicated plasmids, and then treated with FFAs for 24 h and the proteasomal inhibitor MG132 (10 μM) during the last 4 h. The ubiquitination of NRF2 was detected by immunoblotting and immunoprecipitation analysis. (**D**) The half-life of NRF2 protein was determined by pulse-chase assay with the protein synthesis inhibitor CHX (25 μM) administration. $n = 3$. Data are presented as mean ± SEM.

mice (Figure 6E). Furthermore, AAV8-PSA treatment activated the NRF2 antioxidative pathway, enhanced serum β-hydroxybutyrate (mainly derived from fatty acid oxidation) level, and increased the expression of the fatty acid β-oxidation gene PGC1α, while it also decreased the expression of the lipogenesis genes SREBP-1c and PPARγ (Figure 6F–H), consistent with our *in vitro* mechanistic observations. Additionally, we examined glucose metabolism, inflammation, and fibrosis under PSA treatment in *ob/ob* mice. Our results showed that although PSA overexpression (AAV8-PSA) did not significantly influence hepatic gluconeogenesis genes glucose-6-phosphatase (G6Pase) and phosphoenolpyruvate carboxykinase (PEPCK) or the insulin signaling pathway (Supplementary Figure S3), which was consistent with our *in vitro* results, the inflammatory response and liver fibrosis were obviously improved by AAV8-PSA compared with vehicle treatment in *ob/ob* mice, as evidenced by decreased mRNA expression of inflammatory cytokines F4/80, C-C motif chemokine ligand 2 (CCL2), and interleukin-1β (IL-1β) and fibrosis markers transforming growth factor-β (TGF-β), collagen type I α1 (COL1α1), and α-smooth muscle actin (α-SMA) (Figure 6H), attenuated protein levels of TGF-β and α-SMA (Figure 6I), and diminished staining of F4/80 and Sirius Red (Figure 6J), indicating that PSA protected *ob/ob* mice from inflammation and fibrogenesis. In summary, these findings indicate that rescue of PSA mitigates NAFLD development and might be a promising therapeutic approach for this pathological condition.

PSA is a potential marker during the progression of NAFLD in human liver samples

To further characterize the value of PSA expression in the progression of fatty liver diseases, we analyzed human liver tissue microarrays. A total of 78 cases containing 16 normal liver

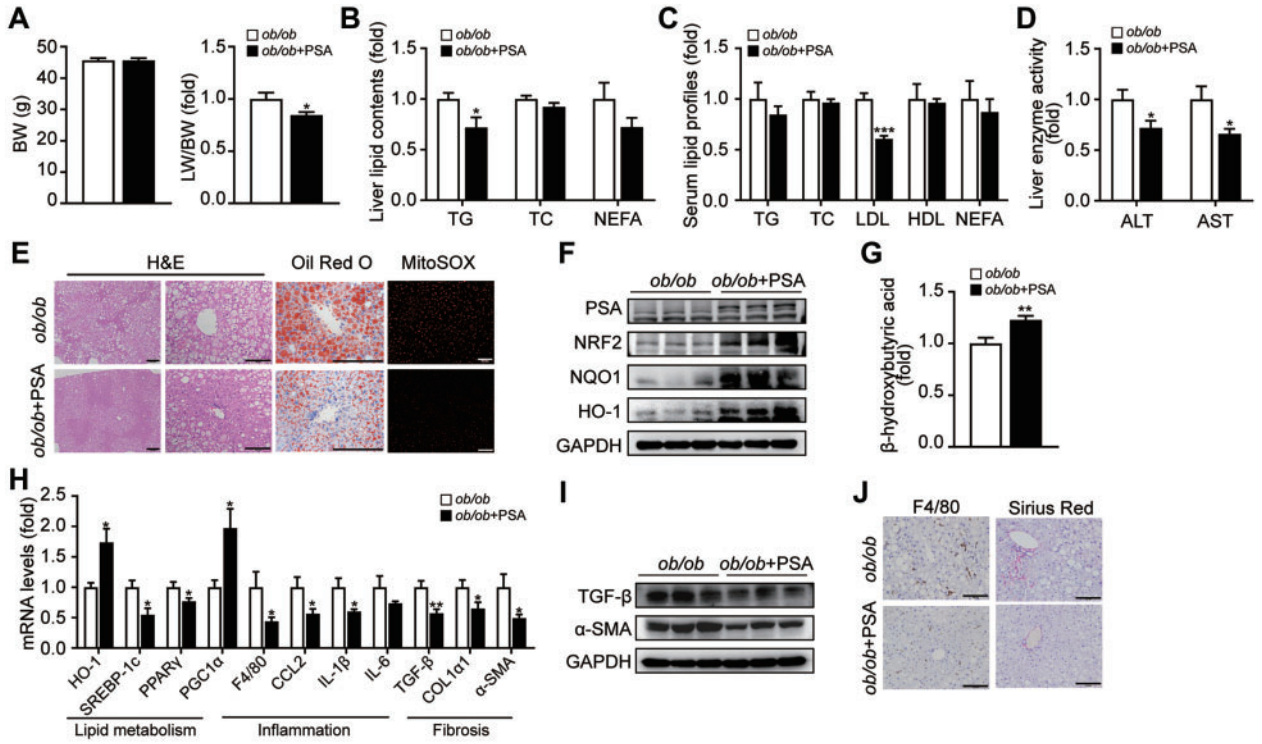

Figure 6 PSA attenuates hepatic steatosis in *ob/ob* mice. The 8-week-old *ob/ob* mice were injected with AAV8-PSA or AAV8-GFP as control via tail vein and examined 4 weeks later. (**A**) BW and the ratio of LW/BW were determined. (**B**) Liver TG, TC, and NEFA were determined enzymatically. (**C** and **D**) The serum lipid profiles (TG, TC, LDL, HDL, and NEFA) and enzyme activities (ALT and AST) were tested enzymatically. (**E**) H&E, Oil red O, and MitoSOX staining of liver sections. (**F**) The protein levels of indicated genes related to the NRF2 signaling pathway were determined by western blotting. (**G**) β-hydroxybutyric acid was tested enzymatically. (**H**) The mRNA levels of indicated genes related to lipid metabolism, inflammatory response, and fibrosis were determined by qRT-PCR. (**I**) The protein levels of indicated genes related to liver fibrosis were determined by western blotting. (**J**) F4/80 IHC and Sirius Red staining of liver sections. Scale bar, 200 or 100 μm. $n = 6$ mice per group. Data are presented as mean ± SEM. $^{*}P < 0.05$, $^{**}P < 0.01$, $^{***}P < 0.001$.

tissues, 7 hepatic steatosis with inflammation, 28 cirrhosis, and 27 hepatocellular carcinomas were analyzed to correlate the expression of PSA with patient clinicopathological features, images of hematoxylin and eosin (H&E) staining and clinical information obtained from www.avilabio.com/public/details?productId=59689&searchText=. Overall, compared with normal liver tissue, fatty liver ($P < 0.05$), cirrhosis ($P < 0.001$), and hepatocellular carcinoma ($P < 0.001$) all showed downregulated PSA expression (Figure 7A and B). In summary, our data suggest that PSA reduction might contribute to enhanced steatosis or even liver cirrhosis and cancer in the human liver and, as such, might be a promising biomarker and a therapeutic target for NAFLD.

Discussion

The incidence of NAFLD has doubled over the past two decades. Currently, no effective drugs are available for NAFLD management in the clinic mainly because the mechanisms underlying the disease are not fully understood. In the present study, we identified PSA as an important metabolic regulator that was suppressed in livers from NAFLD patients and mouse models, and such PSA deficiency stimulated oxidative stress by promoting NRF2 degradation, subsequently leading to excessive hepatic lipid accumulation. Moreover, rescuing PSA attenuated hepatic steatosis, indicating its possibility as a therapeutic target for NAFLD.

Our observations uncovered a crucial role of PSA deficiency in hepatic lipid dysregulation. Analysis of both human and mouse NAFLD samples provided clinical and basic pathological insights into the relationship between decreased PSA and hepatic steatosis, an association that was functionally validated by PSA knockdown in hepatocytes. Notably, lipid accumulation induced by PSA ablation was only seen with the application of FFA, but not under basal conditions. This pattern was similar to that reported for some other crucial genes identified in NAFLD (Fan et al., 2016), indicating that PSA deficiency may be a new genetic background contributor to NAFLD. An increasing amount of evidence suggests that genetic determinants of NAFLD may reinforce the disease phenotype under environmental challenges (Anstee et al., 2016; Stender et al., 2017). Our results demonstrated that PSA knockdown mainly influenced lipogenesis and fatty acid β-oxidation and accelerated TG overload, which has been shown to be the most abundant

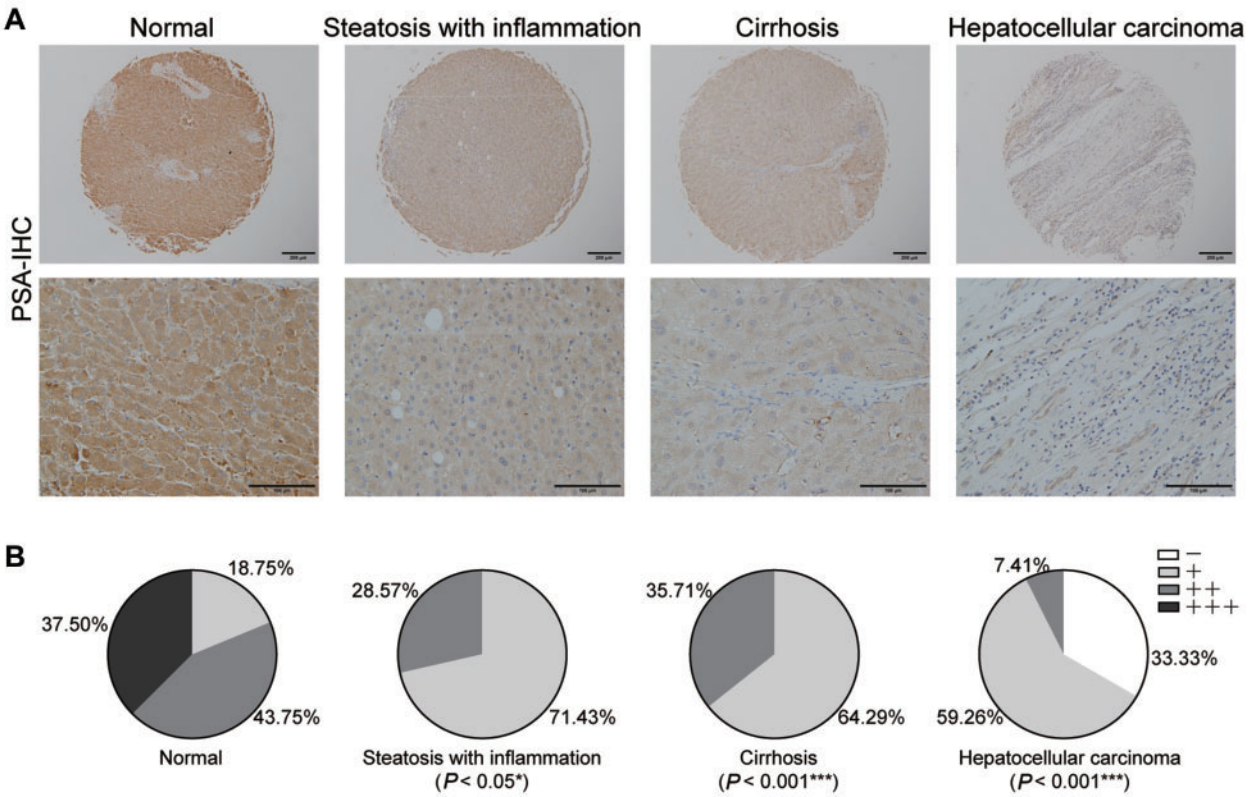

Figure 7 PSA expression is associated with NAFLD progression in human liver samples. Tissue microarrays with 78 cases were used to detect protein expression of PSA by IHC. (**A**) Representative images of livers from normal ($n = 16$), hepatic steatosis with inflammation ($n = 7$), cirrhosis ($n = 28$), and liver cancer ($n = 27$) stained for PSA. Scale bars, 200 or 100 μm. (**B**) All stained tissue sections were semi-quantitatively scored. Fisher's exact test was used to compare normal with each pathologically categorical variable. $^{*}P < 0.05$, $^{***}P < 0.001$.

accumulation contributing to hepatic lipid disorder during NAFLD (Donnelly et al., 2005). Moreover, we found that mitochondrial amount and function were also altered in cultured hepatocytes in the absence of PSA, and the role of PSA in energy metabolism merits exploration in future studies.

We revealed that PSA insufficiency induced oxidative stress by promoting NRF2 degradation, which might represent an undiscovered mechanism for the increased ROS production during NAFLD. Oxidative stress has been critically linked to hepatic lipid homeostasis perturbation (Furukawa et al., 2004; Friedman et al., 2018). We demonstrated that silencing PSA in human hepatocytes induced intracellular ROS mainly through decreasing NRF2, a master regulator of an intracellular antioxidant response by activating an array of genes, including phase II detoxifying enzymes and antioxidants that protect cells from toxic chemicals (Zhang, 2006). Recent studies have revealed a regulatory role of NRF2 by protecting the liver from oxidative stress in NAFLD progression (Bricambert et al., 2018; Azzimato et al., 2020). Our results provide further evidence for this concept and suggest that PSA might be an upstream regulator of NRF2 during this course. Although NRF2 knockdown only showed an increasing trend in intracellular TG accumulation and gene levels of SREBP-1c and PPARγ, as well as a decreasing trend of PGC1α compared with the control group, the differences in the effects induced by PSA overexpression with and without NRF2 knockdown were statistically significant, indicating that the effect of PSA on lipid metabolism was at least partly due to the NRF2 signaling pathway. Moreover, we also revealed that PSA regulated NRF2 degradation via the proteasomal pathway and expanded more candidates to modulate the NRF2 pathway posttranscriptionally.

Our study proposed PSA as a potential therapeutic target for NAFLD. Restoration of PSA expression from the reduced levels seen in the livers of NAFLD patients and mice markedly attenuated TG accumulation and hepatic steatosis in genetically induced *ob/ob* mice. PSA is a member of the M1 aminopeptidase family, which is implicated in the regulation of a wide range of cellular processes such as cell maintenance, development, and apoptosis (Drinkwater et al., 2017). A series of studies have proposed the associations and potential targets of these aminopeptidases in diseases such as malaria (Skinner-Adams et al., 2010), cancer (Watanabe et al., 2003; Reid et al., 2009), and immune-mediated diseases (Stratikos, 2014; Robinson and Brown, 2015). Moreover, our human tissue microarray analysis provided clinicopathological insight into the association of reduced PSA expression and the progression of NAFLD, including cirrhosis and hepatocellular carcinoma. Additionally, the inflammatory response and fibrosis were also improved in

PAS-treated *ob/ob* mice. Since we suggested the therapeutic potential of targeting PSA in hepatic steatosis through counteracting oxidative stress mediated by NRF2, the expression of which has also been reported to decrease gradually in the end stages of human liver diseases (Kurzawski et al., 2012) and the deficiency of which in mice is closely related to fibrosis development (Oh et al., 2012), additional possible effects of PSA in hepatic fibrosis, cirrhosis, and hepatocellular carcinoma will be the subject of further investigations.

In summary, our study identified a novel role of PSA in medicating hepatic TG metabolism by altering fatty acid synthesis and β-oxidation. The antioxidant function of PSA occurs through activation of NRF2 by stabilizing the NRF2 protein, which might represent a new mechanism for the initiation of antioxidant reactions in the liver. Moreover, rescuing hepatic PSA might have therapeutic potential for NAFLD.

Materials and methods

Animals and treatment

All mouse studies were conducted according to protocols approved by the Laboratory Animal Welfare and Ethics Committee of the Army Medical University. Male C57BL/6, *ob/ob*, and *db/db* mice were purchased from the Model Animal Research Center of Nanjing University. HFD models were established by putting mice on an HFD (fat, 60 Kcal%; protein, 20 Kcal%; carbohydrates, 20 Kcal%; Research Diet) continuously for the indicated weeks. All mice were housed with a standard 12-h dark/light cycle with food and water ad libitum. After the animals were sacrificed, the tissues were immediately snap frozen and stored at −80°C or formalin-fixed for subsequent analysis. To evaluate the effects of rescuing PSA, 8-week-old *ob/ob* mice were injected with AAV8-PSA or control vectors (AAV8-GFP) and sacrificed 4 weeks later.

Human tissue samples

The experimental protocols were approved by the Ethics Committee of Xinqiao Hospital and were consistent with the Declaration of Helsinki (Clinical trial register no. ChiCTR-ROC-17010719). All samples were collected from patients hospitalized at Chongqing Medical University, and written consent was obtained from each participant. The procedure was carried out similarly to our previous study (Zheng et al., 2019). Briefly, liver samples were obtained from individuals with NAFLD who underwent percutaneous liver biopsy, and the control was collected from liver transplant donors. The diagnostic criteria for NAFLD were as follows: (i) physical examination, laboratory investigation, and liver biopsy; (ii) other causes of liver diseases were ruled out, such as current or past excessive alcohol consumption (defined as average daily consumption of alcohol >20 g for males or >10 g for females), chronic hepatitis C or hepatitis B, autoimmunity, celiac disease, genetic disorders based on self-reports, or if laboratory and/or histopathological data showed causes of liver disease other than NAFLD. All liver specimens were snap frozen after resection and stored at −80°C.

H&E staining, IHC, and immunofluorescence (IF) analyses, and Sirius Red and Oil red O staining

H&E, IHC, and Oil red O staining were carried out as previously described (Zheng et al., 2019). Briefly, for H&E analysis, tissue sections were prepared using paraffin, and these paraffin sections were subjected to H&E staining. For Oil red O analysis, cells were fixed in formaldehyde solution, and frozen liver sections and cells were subjected to Oil red O staining. For IHC and IF analysis, tissue sections were prepared using paraffin, and these paraffin sections were subjected to IHC or IF staining using the indicated antibodies. Paraffin sections were used for Sirius Red staining with a commercial kit (Solarbio G1470). Digital images were obtained with a light microscope (Olympus).

Cell line and treatment

Huh7 cells were purchased from the Cell Bank of the Chinese Academy of Sciences. Cells were cultured in Dulbecco's Modified Eagle's Medium (DMEM, Gibco) supplemented with 10% fetal bovine serum (FBS, Excell) in a 5% CO_2 incubator at 37°C. All cell identities were confirmed and cultured as recommended by the supplier. Mycoplasma determination was performed by Shanghai Biowing Applied Biotechnology Co.

The cellular lipid accumulation model was induced by FFAs, including palmitate and oleic acid at a final ratio of 1:2, final concentration of 0.2 mM (Sigma-Aldrich), which were added to the medium for 24 h. For knockdown, cells were seeded in 6-well culture plates and transiently transfected with 30 pmol/well of siRNA oligonucleotides with RNAiMAX (Life Technology) according to the manufacturer's instructions. PSA-specific, NRF2-specific, and the corresponding negative control siRNAs were synthesized by RIBOBIO. For overexpression, cells were seeded in 6-well culture plates and transfected with 1 μg plasmid using Lipofectamine 3000 Reagent (Invitrogen) according to the manufacturer's instructions. Plasmids of PSA overexpression and control vector were generated by Sino Biological. Insulin was purchased from Sigma-Aldrich. CHX was purchased from MCE. MG132 was purchased from Santa-Cruz Biotechnology.

MitoTracker Green fluorescence

Cells were seeded with climbing sheets in 12-well culture plates and transfected as stated. To label mitochondria, we incubated cells for 30 min using MitoTracker Green FM (Thermo M7514) at a working concentration of 200 nM. After staining was completed, the staining solution was replaced with fresh prewarmed buffer. Antifluorescence quenching sealing liquid

was used for fixation and mounting. Digital images were obtained with a fluorescence microscope (Olympus).

qRT-PCR

Total mRNA was isolated from cultured cells or tissue samples using TRIzol (TaKaRa) according to the manufacturer's instructions. RNA quality was assessed on a Nanodrop2000, where the 260/280 ratio was obtained. Samples with a ratio of 1.8–2.0 were processed for gene analysis. One microgram of mRNA was reverse-transcribed into cDNA using the PrimeScript RT Reagent Kit with gDNA Eraser (TaKaRa) according to the manufacturer's protocol. SYBR Green (TaKaRa) was applied to quantify PCR amplification. Expression levels were calculated using the ΔCt-method. The mtDNA copy number was assessed using primers specific for the mitochondrial cytochrome c oxidase subunit 2 (COX2) gene and was normalized to genomic DNA using the ribosomal protein s18 (rps18) nuclear gene. The COX2 primer pairs were purchased from BioRad (qHsaCED0048349). The rest of primer pairs used in this study are described in Supplementary Table S1.

Western blotting analysis and antibodies

For protein extraction, cells were lysed in sample buffer (50 mM Tris–HCl, pH 6.8, 2% SDS, 10% glycerol, 100 mM dithiothreitol, and 0.1% bromophenol blue), and tissue lysates were prepared as previously described (Liu et al., 2018). Protein concentrations were measured using the BCA Protein Assay Kit (Beyotime). Extracted protein lysates were resolved by SDS–PAGE and immunoblotted with the indicated primary antibodies (1:500–1:10000) and their corresponding HRP-conjugated secondary antibodies. Blots were developed with chemiluminescent HRP substrate (Millipore) and imaged using a fusion FX5s system (Vilber Lourmat). Antibodies against the following proteins were used: PSA, NRF2, α-SMA, TGF-β, and ATP6 from Abcam; Akt, p-Akt (Ser473), IRS1, p-IRS1 (Ser307), p-IRS1 (Ser895), and F4/80 from Cell Signaling Technology; FASN, SREBP-1, NQO1, HO-1, GCLM, SDHB, COX5B, ATP5A, GAPDH, and β-actin from Santa-Cruz Biotechnology; PGC1α from Novus Biologicals; UQCRC1 and CYTB from Bioss.

Metabolic measurement of OCR

The OCR of Huh7 cells was determined using an Agilent Seahorse XF extracellular flux analyzer (Agilent Technologies) according to our previous description (Liu et al., 2018). Briefly, Huh7 cells were maintained at 60%–80% confluence in XF cell culture plates, and the real-time change in OCR was then monitored following a sequential injection of 1 μM oligomycin, 1 μM carbonyl cyanide 4-(trifluoromethoxy)phenylhydrazone (FCCP), and 0.5 μM rotenone (Hernandez et al., 2021). Data were calculated from three independent measurements obtained prior to or after compound injection.

ROS production assay

MitoSOX red staining was used for liver tissue and hepatocytes for ROS generation assessment according to our previous description (Zheng et al., 2019). Stained images were acquired using a fluorescence microscope (Olympus). For cultured hepatocytes, intracellular ROS production was also determined by the fluorescence of a dichlorofluorescein probe (Invitrogen) and assessed by flow cytometry according to the manufacturer's instructions.

GSH/GSSG measurement

The rate of chromogenic 5-thio-2-nitrobenzoic acid (TNB) formation from the nonchromogenic substrate 5,5′-dithio-bis-(2-nitrobenzoic acid) (DTNB) correlates to the amount of GSH present and can be measured at 412 nm. Cellular GSH/GSSG levels were measured by using a commercial GSH/GSSG detection kit (Beyotime) according to the manufacturer's protocol.

Immunoprecipitation

For immunoprecipitation, cell lysates were collected at 48 h posttransfection in RIPA buffer containing 10 mM sodium phosphate (pH 8.0), 150 mM NaCl, 1% Triton X-100, 1% sodium deoxycholate, and 0.1% SDS, with the addition of 1 mM dithiothreitol, 1 mM phenylmethylsulfonyl fluoride (PMSF), and protease inhibitor cocktail (PIC). Cell lysates were incubated with 1 μg of antibody with 10 μl of protein A-agarose beads on a rotator at 4°C overnight. The immunoprecipitated complexes were washed and eluted in sample buffer by boiling for 5 min. The samples were then resolved by SDS–PAGE and transferred onto nitrocellulose membranes for immunoblotting analysis. The PSA antibody was purchased from Santa-Cruz Biotechnology.

Ubiquitination and protein half-life analysis

Ubiquitination and half-life assays were performed according to our previous protocol (Zheng et al., 2019). Briefly, for the ubiquitination assay, cells were transfected with the indicated siRNA/plasmids with hemagglutinin (HA)-tagged ubiquitin for 24 h and then treated with FFA. MG132 (10 μM) was added to block proteasome degradation at 4 h before harvest. Cells were lysed and boiled immediately to inactivate cellular ubiquitin hydrolases to preserve ubiquitin–protein conjugates. The lysates were incubated with anti-NRF2 antibody or IgG at 4°C overnight, and immunoprecipitated proteins were analyzed by immunoblotting with an antibody directed against the HA

epitope. To measure the NRF2 protein half-life, cells were treated with PSA plasmid and FFA, and then CHX (25 μM) was added to block protein synthesis. Total lysates were collected at the indicated time points after CHX administration and subjected to immunoblotting analysis.

Metabolic and liver function assays

The levels of TG, total cholesterol (TC), nonesterified fatty acid (NEFA), LDL, high-density lipoprotein cholesterol (HDL), ALT, and AST were measured using their corresponding commercial determination kits (all from Nanjing Jiancheng) with liver tissue or serum samples. Serum β-hydroxybutyric acid concentrations were measured using an ELISA kit from MSK Bio. Cellular TG levels were measured using a commercial TG Quantification Colorimetric kit (Applygen) according to the manufacturer's protocol.

Human liver tissue microarray chips

Human liver tissue microarray chips were purchased from Avilabio (DC-Liv00009); for scanned images of H&E staining, corresponding clinical information, and ethical materials, please refer to http://www.avilabio.com/public/details?productId=59689&searchText=. A total of 78 cases containing 16 normal liver tissues, 7 fatty degeneration with inflammation, 28 cirrhosis, and 27 hepatocellular carcinomas were analyzed. The stained slides were scored as described previously (Kleiner et al., 2005; Jiang et al., 2010), considering (i) the percentage of positive cells (P) grouped into five categories, i.e. 0 (<5%), 1 (5%–25%), 2 (25%–50%), 3 (50%–75%), 4 (75%–100%), and (ii) staining intensity (I) grouped into four categories (color from light to dark), i.e. 0, 1, 2, 3. The score was calculated as (P × I) and divided into four grades: − (0–1), + (2–4), ++ (5–8), +++ (9–12).

Statistical analyses

All data were analyzed using GraphPad Prism 7 (Macintosh). Quantitative values are presented as mean ± SEM. Statistical differences between two experimental groups were analyzed by the two-tailed Student's *t*-test. For comparisons of more than two groups, one-way ANOVA followed by Tukey's multiple comparison tests were performed. For semiquantitative scoring of human liver tissue microarrays, Fisher's exact test was used (SPSS 22.0). Data were considered statistically significant when $P < 0.05$.

Supplementary material

Supplementary material is available at *Journal of Molecular Cell Biology* online.

Funding

This work was supported by the National Natural Science Foundation of China (82070881, 82070836, and 81970752), the National Science Fund for Distinguished Young Scholars (81925007), and the 'Talent Project' of Army Medical University (2017R013, 2019R047, and 2019XQYYYJ003-2).

Conflict of interest: none declared.

Author contributions: B.H., X.X., L.Z., and X.L.: acquisition of data and statistical analysis; B.H., Y.W., Y.L., X.G., and Q.S.: analysis and interpretation of data; Y.Z.: drafting of the manuscript; H.Q., H.Z., and Y.Z.: critical revision of the manuscript for important intellectual content; H.Z. and Y.Z.: study concept and design, obtaining study funding, and study supervision.

References

Adams, L.A., Lymp, J.F., St Sauver, J., et al. (2005). The natural history of nonalcoholic fatty liver disease: a population-based cohort study. Gastroenterology *129*, 113–121.

Alponti, R.F., Alves, P.L., and Silveira, P.F. (2016). Novel adipocyte aminopeptidases are selectively upregulated by insulin in healthy and obese rats. J. Endocrinol. *228*, 97–104.

Anstee, Q.M., Seth, D., and Day, C.P. (2016). Genetic factors that affect risk of alcoholic and nonalcoholic fatty liver disease. Gastroenterology *150*, 1728–1744.e7.

Anstee, Q.M., Targher, G., and Day, C.P. (2013). Progression of NAFLD to diabetes mellitus, cardiovascular disease or cirrhosis. Nat. Rev. Gastroenterol. Hepatol. *10*, 330–344.

Azzimato, V., Jager, J., Chen, P., et al. (2020). Liver macrophages inhibit the endogenous antioxidant response in obesity-associated insulin resistance. Sci. Transl. Med. *12*, eaaw9709.

Baiceanu, A., Mesdom, P., Lagouge, M., et al. (2016). Endoplasmic reticulum proteostasis in hepatic steatosis. Nat. Rev. Endocrinol. *12*, 710–722.

Bhutani, N., Venkatraman, P., and Goldberg, A.L. (2007). Puromycin-sensitive aminopeptidase is the major peptidase responsible for digesting polyglutamine sequences released by proteasomes during protein degradation. EMBO J. *26*, 1385–1396.

Bricambert, J., Alves-Guerra, M.C., Esteves, P., et al. (2018). The histone demethylase Phf2 acts as a molecular checkpoint to prevent NAFLD progression during obesity. Nat. Commun. *9*, 2092.

Champier, J., Jouvet, A., Rey, C., et al. (2005). Identification of differentially expressed genes in human pineal parenchymal tumors by microarray analysis. Acta Neuropathol. *109*, 306–313.

Clark, J.M. (2006). The epidemiology of nonalcoholic fatty liver disease in adults. J. Clin. Gastroenterol. *40(Suppl 1)*, S5–S10.

Constam, D.B., Tobler, A.R., Rensing-Ehl, A., et al. (1995). Puromycin-sensitive aminopeptidase. Sequence analysis, expression, and functional characterization. J. Biol. Chem. *270*, 26931–26939.

Donnelly, K.L., Smith, C.I., Schwarzenberg, S.J., et al. (2005). Sources of fatty acids stored in liver and secreted via lipoproteins in patients with nonalcoholic fatty liver disease. J. Clin. Invest. *115*, 1343–1351.

Drinkwater, N., Lee, J., Yang, W., et al. (2017). M1 aminopeptidases as drug targets: broad applications or therapeutic niche? FEBS J. *284*, 1473–1488.

Fan, Y., Lu, H., Guo, Y., et al. (2016). Hepatic transmembrane 6 superfamily member 2 regulates cholesterol metabolism in mice. Gastroenterology *150*, 1208–1218.

Friedman, S.L., Neuschwander-Tetri, B.A., Rinella, M., et al. (2018). Mechanisms of NAFLD development and therapeutic strategies. Nat. Med. *24*, 908–922.

Furukawa, S., Fujita, T., Shimabukuro, M., et al. (2004). Increased oxidative stress in obesity and its impact on metabolic syndrome. J. Clin. Invest. *114*, 1752–1761.

Gao, G.P., Alvira, M.R., Wang, L., et al. (2002). Novel adeno-associated viruses from rhesus monkeys as vectors for human gene therapy. Proc. Natl Acad. Sci. USA *99*, 11854–11859.

Gil, M., Ramil, F., and Agls, J.A. (2020). Hydroids (Cnidaria, Hydrozoa) from Mauritanian coral mounds. Zootaxa *4878*, zootaxa.4878.3.2.

Hayes, J.D., and Dinkova-Kostova, A.T. (2014). The Nrf2 regulatory network provides an interface between redox and intermediary metabolism. Trends Biochem. Sci. *39*, 199–218.

Hernandez, S., Simoni-Nieves, A., Gerardo-Ramirez, M., et al. (2021). GDF11 restricts aberrant lipogenesis and changes in mitochondrial structure and function in human hepatocellular carcinoma cells. J. Cell. Physiol. *236*, 4076–4090.

Jiang, T., Chen, N., Zhao, F., et al. (2010). High levels of Nrf2 determine chemoresistance in type II endometrial cancer. Cancer Res. *70*, 5486–5496.

Karsten, S.L., Sang, T.K., Gehman, L.T., et al. (2006). A genomic screen for modifiers of tauopathy identifies puromycin-sensitive aminopeptidase as an inhibitor of tau-induced neurodegeneration. Neuron *51*, 549–560.

Kawano, Y., and Cohen, D.E. (2013). Mechanisms of hepatic triglyceride accumulation in non-alcoholic fatty liver disease. J. Gastroenterol. *48*, 434–441.

Kleiner, D.E., Brunt, E.M., Van Natta, M., et al. (2005). Design and validation of a histological scoring system for nonalcoholic fatty liver disease. Hepatology *41*, 1313–1321.

Koliaki, C., Szendroedi, J., Kaul, K., et al. (2015). Adaptation of hepatic mitochondrial function in humans with non-alcoholic fatty liver is lost in steatohepatitis. Cell Metab. *21*, 739–746.

Kurzawski, M., Dziedziejko, V., Urasinska, E., et al. (2012). Nuclear factor erythroid 2-like 2 (Nrf2) expression in end-stage liver disease. Environ. Toxicol. Pharmacol. *34*, 87–95.

Liu, X., Qu, H., Zheng, Y., et al. (2018). Mitochondrial glycerol 3-phosphate dehydrogenase promotes skeletal muscle regeneration. EMBO Mol. Med. *10*, e9390.

Mansouri, A., Gattolliat, C.H., and Asselah, T. (2018). Mitochondrial dysfunction and signaling in chronic liver diseases. Gastroenterology *155*, 629–647.

Oh, C.J., Kim, J.Y., Min, A.K., et al. (2012). Sulforaphane attenuates hepatic fibrosis via NF-E2-related factor 2-mediated inhibition of transforming growth factor-β/Smad signaling. Free Radic. Biol. Med. *52*, 671–682.

Pessayre, D. (2007). Role of mitochondria in non-alcoholic fatty liver disease. J. Gastroenterol. Hepatol. *22(Suppl 1)*, S20–S27.

Petrosillo, G., Portincasa, P., Grattagliano, I., et al. (2007). Mitochondrial dysfunction in rat with nonalcoholic fatty liver involvement of complex I, reactive oxygen species and cardiolipin. Biochim. Biophys. Acta *1767*, 1260–1267.

Reid, A.H., Protheroe, A., Attard, G., et al. (2009). A first-in-man phase I and pharmacokinetic study on CHR-2797 (Tosedostat), an inhibitor of M1 aminopeptidases, in patients with advanced solid tumors. Clin. Cancer Res. *15*, 4978–4985.

Ren, G., Ma, Z., Hui, M., et al. (2011). Cu, Zn-superoxide dismutase 1 (SOD1) is a novel target of Puromycin-sensitive aminopeptidase (PSA/NPEPPS): PSA/NPEPPS is a possible modifier of amyotrophic lateral sclerosis. Mol. Neurodegener. *6*, 29.

Robinson, P.C., and Brown, M.A. (2015). ERAP1 biology and assessment in Ankylosing Spondylitis. Proc. Natl Acad. Sci. USA *112*, E1816.

Samuel, V.T., and Shulman, G.I. (2012). Mechanisms for insulin resistance: common threads and missing links. Cell *148*, 852–871.

Skinner-Adams, T.S., Stack, C.M., Trenholme, K.R., et al. (2010). Plasmodium falciparum neutral aminopeptidases: new targets for anti-malarials. Trends Biochem. Sci. *35*, 53–61.

Stender, S., Kozlitina, J., Nordestgaard, B.G., et al. (2017). Adiposity amplifies the genetic risk of fatty liver disease conferred by multiple loci. Nat. Genet. *49*, 842–847.

Stratikos, E. (2014). Regulating adaptive immune responses using small molecule modulators of aminopeptidases that process antigenic peptides. Curr. Opin. Chem. Biol. *23*, 1–7.

Utzschneider, K.M., and Kahn, S.E. (2006). Review: the role of insulin resistance in nonalcoholic fatty liver disease. J. Clin. Endocrinol. Metab. *91*, 4753–4761.

Vomund, S., Schafer, A., Parnham, M.J., et al. (2017). Nrf2, the master regulator of anti-oxidative responses. Int. J. Mol. Sci. *18*, 2772.

Watanabe, Y., Shibata, K., Kikkawa, F., et al. (2003). Adipocyte-derived leucine aminopeptidase suppresses angiogenesis in human endometrial carcinoma via renin–angiotensin system. Clin. Cancer Res. *9*, 6497–6503.

Zhang, D.D. (2006). Mechanistic studies of the Nrf2–Keap1 signaling pathway. Drug Metab. Rev. *38*, 769–789.

Zheng, Y., Qu, H., Xiong, X., et al. (2019). Deficiency of mitochondrial glycerol 3-phosphate dehydrogenase contributes to hepatic steatosis. Hepatology *70*, 84–97.